Available online at www.sciencedirect.com
SCIENCE DIRECT®
International Journal of Thermal Sciences 45 (2006) 475–486
International Journal of Thermal Sciences
www.elsevier.com/locate/ijts

Turbulent thermophoresis effect on particle transport processes

C.H. Chiu, C.M. Wang, M.C. Chiou *

Department of Vehicle Engineering, National Huwei University of Technology, Yunlin, Taiwan

Received 19 March 2004; received in revised form 27 December 2004; accepted 7 March 2005
Available online 19 December 2005

Abstract

The analytical solutions have been obtained with the aid of the surface rejuvenation model for the quantitative predictions of mean eddy approach distance, mean thermophoretic velocity and mean thermophoretic transport rate in detail. The mean sublayer residence time solved in accordance with the velocity distribution in the fully turbulent fluid flow is consistent with visual observations. The local cumulative submicron particle transport rate has been theoretically predicted including the conjoint effects of eddy diffusion, Brownian diffusion, and thermophoretic effect. The results give an explanation for the complex phenomena of the comparable coupling between the thermal and turbulent mechanism during the time intervals of successive eddies, especially for the heating surface. A good agreement of dimensionless mean transport rate in an isothermal turbulence fluid flow proves the subsequent developments of the coupling on the particle transfer mechanisms in the viscous sublayer.
© 2005 Elsevier SAS. All rights reserved.

Keywords: Surface rejuvenation model; Turbulence; Transport parameter; Dimensionless mean eddy approach distance; Dimensionless; Dimensionless mean thermophoretic velocity; Dimensionless mean thermophoretic transport rate

1. Introduction

In many industries the composition of processing gases may contain any of an unlimited range of particulate, liquid, or gaseous contaminants and may be influenced by uncontrolled factors of temperature and humidity. When such an impure gas is bounded by a solid surface, a boundary layer will develop and the energy and momentum transfer gives rise to temperature and velocity gradients. Mass transfer caused by gravitation, molecular diffusion, eddy diffusion, and inertial impact results in deposition of the suspended components onto the surface. A number of engineering fields involve droplet and particle deposition, and may exploit or suppress the deposition depending on the practical requirement. For example, the application of pigments, ceramic powders to surfaces, chemical coating of metals, and filtration all seek more efficient ways of increasing deposition, whereas the deposition of aerosol particles appears as an unwanted phenomenon in the contamination of semiconductor elements during manufacture, soiling of artistic products and indoor surfaces, fouling and corrosion of heat exchangers, boiler tubes, turbine equipment, etc.

In most engineering situations particle transport occurs in the presence of turbulent flow and the addition of particulate matter to turbulent flows increases the complexity of the phenomena. Therefore, any models should represent the behavior of flow in the wall region as accurately as possible. The particle tracking methods are Lagrangian approach which treats trajectories of individual particles, and Eulerian approach which views the aerosol particle system as a continuum phase and treats them as a species concentration field [1–4]. The viscous sublayer models relied on the surface renewal, penetration and surface rejuvenation concepts indicate that the processes in the region near the wall mainly determine the momentum, heat and mass transfer. The fluid motion led to an acceleration of the low momentum fluid near the wall, and it has been suggested that the low momentum fluid near the wall leads to a laminar boundary being developed and which eventually becomes

* Corresponding author.
E-mail address: achi@sunws.nhit.edu.tw (M.C. Chiou).

1290-0729/$ – see front matter © 2005 Elsevier SAS. All rights reserved.
doi:10.1016/j.ijthermalsci.2005.03.010

Nomenclature

C	particle concentration
C_f	Cunningham slip correction factor
C_m	momentum exchange coefficient
C_s	thermal slip coefficient
C_t	temperature jump coefficient
d	pipe diameter
D	molecular diffusivity
d_p	particle diameter
$f(y)$	initial profile of rejuvenation
$h(y)$	initial profile of rejuvenation
H	instantaneous eddy approach distance
k	thermophoretic coefficient
K_g	thermal conductivity of carried gas
K_n	Knudsen number
K_p	thermal conductivity of particle
p_f	statistic distribution for f
p_h	statistic distribution for h
p_H	statistic distribution for H
Pr	Prandtl number
p_τ	statistic distribution for τ
Re	Reynolds number
Sc	Schmidt number
T	temperature
u	axial velocity
U	unit step function
V_d	thermophoretic transport rate
V_t	thermophoretic velocity
V_{th}	dimensionless mean thermophoretic velocity
y	distance from wall
Y	dimensionless distance $= y/d$

Greek letters

α	thermal diffusivity
ν	kinematic viscosity
υ	transport parameter, $= \overline{H}/\sqrt{\nu\bar{\tau}}$
ϑ	transport parameter, $= \overline{H}/\sqrt{\alpha\bar{\tau}}$
ω	transport parameter, $= \overline{H}/\sqrt{D\bar{\tau}}$
ϖ	transport parameter, $= \sqrt{(2\omega)^2 + (V_{\text{th}}\omega^2/\vartheta^2)^2}$
$\Im$	kinematic viscosity or thermal diffusivity
$\Re$	dimensionless mean approach distance, $= \overline{H}/d$
τ	residence time of sublayer
ϕ	Axial velocity or temperature fraction
σ	shear stress

Superscripts

$+$	Dimensionless parameters
$\overline{\ }$	mean with respect to statistic distributions
$\sim$	mean with respect to p_τ

Subscripts

∞	bulk stream conditions
w	wall conditions

unstable, leading to a sudden ejection of fluid away from the wall. The visual flow studies of the turbulent fluid flow close to the wall clearly demonstrated that eddies continuously penetrate deep into the wall region resulting in an unsteady flow there [5], and that the particles suspended in turbulent fluid are transported by the bursting events of the wall regions in which the values of turbulent intensities and Reynolds stresses increase at lager particles ($d_p = 1100$ μm) and decrease at smaller particles ($d_p = 120$ μm) depended on the number of wall ejections [6]. The surface rejuvenation model has modified the basic surface renew model, which is based on the assumption that turbulent eddies move from main flow into direct contact with the wall and contradicts the observation from the experimental studies, to account for the effect of eddies not penetrating down to the wall itself [7] and has been coupled with a stochastic computational concept to determine the mean mass transfer coefficient in terms of unspecified parameters of eddy lifetime and approach distance [8] and to evaluate turbulent convection transfer in the viscous sublayer by adjusting its parameters [9–11].

In a gas–solid mixture the particles move with the air stream and arrive at the edge of the viscous sublayer by turbulent eddy diffusion. The convection by the bulk flow plays an important role for all particle sizes. Small particles are transported through the sublayer by molecular diffusion, especially close to a wall where the concentration gradients are large. The inertia of larger particles on entering the sublayer is sufficiently great, deposition will occur by inertial and sedimentary mechanism. One particular area concerns the thermophoretic phenomenon, which is the movement of aerosol particles with a variable velocity toward the region of lower temperature since the molecular bombardment of particles is more energetic on the hot side than on the cold side. Experimental results show that thermophoresis plays an important role in the migration of small particles provided $d_p < 1.0$ μm [12]. Goren [13] was the first one to theoretically demonstrate that the solid particle deposition onto a cold solid wall in the presence of thermophoretic effect. The numerical results of thermal deposition of aerosol particles on a flat body indicate that the deposition flux decreases with increasing surface temperature and increases nonlinearly with increasing thermophoretic coefficients [14]. Modeling clusters deposition in the thermal plasma flash evaporation process shows that the concentration boundary layer is significantly suppressed by the thermophoretic force, and that the thermophoresis plays a dominate role than that of diffusion giving rise to an uniform deposition efficiency for different cluster sizes (1–10 nm) [15]. An experimental measurement of the thermophoretic deposition of submicron particles on the smooth wall of a circular rod and a simple

approximation of a two-dimensional method for predicting the thermophoretic effects on submicron particles has been introduced [16]. A plate-to-plate thermal precipitation system investigated the deposition of agglomerate submicron particles for diesel engine exhaust gas treatment expresses that the deposition efficiencies are nearly independent of particle size and Knudsen number for particle size range of 34–300 nm, and that a constant thermophoretic coefficient $k = 0.55$ derived by Waldmann and Schmitt [17] for the free molecular regime can also be applied for agglomerate soot particles in the transition regime [18]. A numerical investigation of thermophoretic efficiency at the entrance region of a circular tube found that the deposition efficiency is higher at the entrance region than that of fully developed flow [19].

In spite of gradual progress, effort is still required to improve the prediction of transport processes in the nonisothermal turbulence flow field. The surfaces renew and penetration model has been modified for predicting the local cumulative submicron particle deposition from a turbulent flow onto a tube wall [20]. Although this model is based on the somewhat simplistic assumption, it does validate that the influence of the mean axial pressure gradient on the viscous sublayer becomes important for the molecular diffusion associated with low Reynolds number flow. Because of the potential usefulness of surface rejuvenation concept in the analysis of turbulent convection transport processes, an analytical approach to the formulation of this concept is presented in this paper, where the stochastic form for the turbulent heat and mass transfer processes is extended to involve the effects of molecular diffusion, turbulence, and thermophoretic effect. Because the interaction of thermal and turbulent mechanism in front of the solid wall is expected to have a significant effect on the particulate matter transport, the thermophoretic velocity is analyzed in detail and the physical trends of the comparable effects of turbulent intensity, and thermophoretic effect on particle transport process are quantitatively revealed in some extent. It is helpful to explain some of limited fouling data, which have been reported, and to understand the complex phenomena of the interaction between suspended particulate matter and the turbulence of the carrier fluid in nonisothermal boundary layers.

2. Assumptions and limitations

The turbulent eddy at the outer edge of the sublayer is intermittent and the oscillating turbulent velocity components cause the fairly sharp boundaries that fluctuate strongly with time. As long as the transfer of particle suspended in the main flow is concerned, the turbulent mixing motion is responsible not only for an exchange of momentum, but it also enhances the particle transfer in the flow fields associated with the concentration distribution. Namely, the uniform distribution of concentration intermittently moved with turbulent eddy can be changed from a deterministic quantity to a random variable because the concentration gradient will be momentarily steeper near the fresh fluid during a random distribution of eddy lifetimes.

The particles moving under fully developed turbulent flow conditions are transported from one location to another relative to the random eddy variation of carrier fluid. The flow of spherical and dilute particles suspended in a turbulent carrier fluid is considered and the collisions between particles are neglected. Thus, the sedimentation of particles is not included as compared with particle diffusivities. The fluid motion is unaffected by the presence of the dilute particles so that the concentration equation can be decoupled from the momentum and energy equations where the fluid temperature and velocity distribution are calculated independently due to the temperature development caused by the radial turbulence gradient is analogous to the oscillating sublayer development.

The present attempt is to create a mathematical basis for the investigation of the particle transport in the turbulent boundary layer flows with the aid of semi-empirical hypotheses. As the consideration is restricted to the viscous sublayer, the transfer processes are directly affected by the conditions adjacent to the wall. The problem can be simplified by stipulating that the flow in the boundary layer of a tube is regarded as an approximation to parallel flow where the dependence of the mean velocity in the main flow on the longitudinal direction is very smaller than that on the transverse direction. Neglecting the effects of viscous dissipation and pressure gradient, the mechanisms of molecular diffusion, temperature gradient, and turbulent intensity are assumed to dominate the particle transfer onto an isothermal stagnation surface, which is immersed in the fluid of constant velocity and temperature.

3. Theoretical approach

A viscous sublayer close to the wall is assumed to be generated randomly by the inrushing fluid which has average values of velocity, u_∞, temperature, T_∞, and concentration, C_∞. The fluid elements intermittently move from mainstream to within various small distances H of the surface where the fluid in the immediate vicinity of the wall is a discontinuously viscous sublayer. Unsteady momentum, heat and mass transfers are assumed to govern the area within the wall region for the period of time between two successive eddies. A sketch of the periodically developing sublayer flow is presented in Fig. 1. In which the transformation of instantaneous properties into the lifetime of a single eddy can be achieved by substituting the residence time, τ, between successive eddies for the instantaneous contact time of a single eddy, and thus the unsteady distributions of an individual element of fluid with constant properties can be described by the boundary layer equations of the form

$$\frac{\partial \phi}{\partial \tau} = \Im \frac{\partial^2 \phi}{\partial y^2}, \qquad \frac{\partial C}{\partial \tau} = D \frac{\partial^2 C}{\partial y^2} - V_t \frac{\partial C}{\partial y} \tag{1}$$

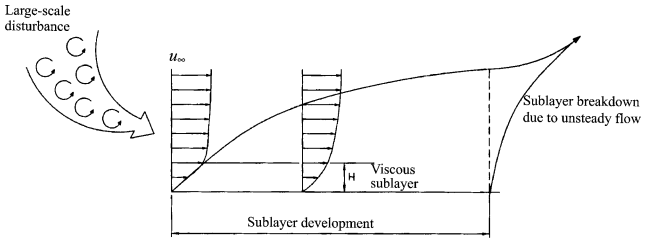

Fig. 1. Developing sublayer patch at the tube wall during the residence time τ between two successive eddies.

where ϕ represents the axial velocity and temperature fraction, $\Im$ the kinematic viscosity and thermal diffusivity, and y the distance measured normal to the surface. C is the particle concentration, and D the particle diffusivity given by the Einstein equation $D = 1.38 \times 10^{-23} T/3\pi\mu d_p$ where T is the absolute temperature, d_p the particle diameter. The initial and boundary conditions are given for a specified wall concentration C_w by

$$\begin{aligned}
&\phi = \phi_\infty\big[U(y-H)\big] + f(y)\big[1-U(y-H)\big]\\
&C = C_\infty\big[U(y-H)\big] + h(y)\big[1-U(y-H)\big] \quad \text{at } \tau = 0\\
&\phi = \phi_w, \quad C = C_w \quad \text{at } y = 0\\
&\phi = \phi_\infty, \quad C = C_\infty \quad \text{at } y \to \infty
\end{aligned} \tag{2}$$

where $f(y)$ and $h(y)$ are the initial profiles in the influenced layer between the wall and the instantaneous approach distance from the surface H, which are identical to the instantaneous profiles just before the preceding rejuvenation. The residence time τ between successive eddies is exponentially distributed with corresponding distribution density function [21]. It has been found that the form of the distribution density functions of the residence time τ over the surface did not appear greatly to affect calculated profile [22], and that the surface renewal models were only slightly influenced by the shape of the distribution of the time interval τ [23, 24]. Some predictions indicate that the distance of surface H strongly depends upon the selection for the distribution density function [7,8]. For the convenient, the random distribution density function, $p_\tau(\tau) = 1/\bar{\tau}e^{-\tau/\bar{\tau}}$, proposed by [21] has been used to predict the mean transport properties, where $\bar{\tau}$ is the mean residence time of sublayer such as the mean time interval between two successive eddies. Analogical forms of $p_f(f) = 1/\bar{f}e^{-f/\bar{f}}$ and $p_H(H) = 1/\overline{H}e^{-H/\overline{H}}$ have been found in correspondence with experimental data for predicting the mean transport properties of $f(y)$ and H respectively [23]. Therefore, Eq. (1) can be transformed into its mean domain by multiplying each term with the distribution density functions and then integrating, i.e.

$$\begin{aligned}
&\bar{\phi} - \bar{f}e^{-y/\overline{H}} - \phi_\infty\big(1-e^{-y/\overline{H}}\big) = \Im\bar{\tau}\frac{\mathrm{d}^2\bar{\phi}}{\mathrm{d}y^2}\\
&\overline{C} - \bar{h}e^{-y/\overline{H}} - C_\infty\big(1-e^{-y/\overline{H}}\big) = D\bar{\tau}\frac{\mathrm{d}^2\overline{C}}{\mathrm{d}y^2} - \overline{V}_t\bar{\tau}\frac{\mathrm{d}\overline{C}}{\mathrm{d}y}
\end{aligned} \tag{3}$$

where

$$\bar{\phi} = \int_0^\infty \frac{1}{\overline{H}}e^{-H/\overline{H}}\int_0^\infty \frac{1}{\bar{f}}e^{-f/\bar{f}}\int_0^\infty \phi\frac{1}{\bar{\tau}}e^{-\tau/\bar{\tau}}\,\mathrm{d}\tau\,\mathrm{d}f\,\mathrm{d}H$$

$$\overline{C} = \int_0^\infty \frac{1}{\overline{H}}e^{-H/\overline{H}}\int_0^\infty \frac{1}{\bar{f}}e^{-f/\bar{f}}\int_0^\infty C\frac{1}{\bar{\tau}}e^{-\tau/\bar{\tau}}\,\mathrm{d}\tau\,\mathrm{d}f\,\mathrm{d}H$$

$\bar{f}(y)$ and $\bar{h}(y)$ are the mean profiles at the end of the time intervals τ. Since the distribution of the time starting from the last instant of the preceding eddy is identical to that of the time interval τ, the use of Danckwert's random contact time distribution and residence time distribution results in $\bar{f}(y) = \bar{\phi}(y)$ and $\bar{h}(y) = \overline{C}(y)$ which reveal that the mean profiles at the end of the time intervals are identical to the mean profiles that are averaged out over the time intervals. The equations are therefore be reduced to

$$\begin{aligned}
&(\bar{\phi} - \phi_\infty)\big(1-e^{-y/\overline{H}}\big) = \Im\bar{\tau}\frac{\mathrm{d}^2\bar{\phi}}{\mathrm{d}y^2}\\
&(\overline{C} - C_\infty)\big(1-e^{-y/\overline{H}}\big) = D\bar{\tau}\frac{\mathrm{d}^2\overline{C}}{\mathrm{d}y^2} - \overline{V}_t\bar{\tau}\frac{\mathrm{d}\overline{C}}{\mathrm{d}y}
\end{aligned} \tag{4}$$

and the boundary conditions become

$$\begin{aligned}
&\bar{\phi} = \phi_w, \quad \overline{C} = C_w \quad \text{at } y = 0\\
&\bar{\phi} = \phi_\infty, \quad \overline{C} = C_\infty \quad \text{at } y \to \infty
\end{aligned} \tag{5}$$

Eqs. (4) and (5) represent the basis of desired surface rejuvenation for mean transport. Substituting $Z = e^{-y/2\overline{H}}$, $\bar{\varphi} = \bar{\phi} - \phi_\infty$ and $\overline{\Phi} = \overline{C} - C_\infty$ into Eq. (4), the acquainted expressions recognized as the Bessel differential equations of order $2\overline{H}/\sqrt{\Im\bar{\tau}}$ and $\sqrt{(2\overline{H}/\sqrt{D\bar{\tau}})^2 + (\overline{H}\overline{V}_t/D)^2}$ can be obtained, and thus the general solutions are

$$\begin{aligned}
\bar{\varphi} &= A_1 J_{2\overline{H}/\sqrt{\Im\bar{\tau}}}(\varsigma) + A_2 Y_{2\overline{H}/\sqrt{\Im\bar{\tau}}}(\varsigma)\\
\overline{\Phi} &= B_1\xi^{-\overline{H}\overline{V}_t/D} J_{\sqrt{(2\overline{H}/D\bar{\tau})^2+(\overline{H}\overline{V}_t/D)^2}}(\xi)\\
&\quad + B_2\xi^{-\overline{H}\overline{V}_t/D} Y_{\sqrt{(2\overline{H}/D\bar{\tau})^2+(\overline{H}\overline{V}_t/D)^2}}(\xi)
\end{aligned} \tag{6}$$

where $\varsigma = 2\overline{H}/\sqrt{\Im\bar{\tau}}Z$ and $\xi = 2\overline{H}/\sqrt{D\bar{\tau}}Z$ are the additional substitutions. According to the corresponding boundary conditions

$$\begin{aligned}
&\bar{\varphi} = \phi_w - \phi_\infty \quad \text{at } \varsigma = \frac{2\overline{H}}{\sqrt{\Im\bar{\tau}}}\\
&\overline{\Phi} = C_w - C_\infty \quad \text{at } \xi = \frac{2\overline{H}}{\sqrt{D\bar{\tau}}}\\
&\bar{\varphi} = 0 \quad \text{at } \varsigma = 0\\
&\overline{\Phi} = 0 \quad \text{at } \xi = 0
\end{aligned} \tag{7}$$

the simple analytic solutions are obtained

$$\bar{\varphi} = (\phi_w - \phi_\infty)\frac{J_{2\overline{H}/\sqrt{\Im\bar{\tau}}}(\varsigma)}{J_{2\overline{H}/\sqrt{\Im\bar{\tau}}}(2\overline{H}/\sqrt{\Im\bar{\tau}})}$$

$$\overline{\Phi} = (C_w - C_\infty)\left(\frac{\xi}{2\overline{H}/\sqrt{D\bar{\tau}}}\right)^{-\overline{H}\overline{V}_t/D} \times \frac{J_{\sqrt{(2\overline{H}/\sqrt{D\bar{\tau}})^2+(\overline{H}\overline{V}_t/D)^2}}(\xi)}{J_{\sqrt{(2\overline{H}/\sqrt{D\bar{\tau}})^2+(\overline{H}\overline{V}_t/D)^2}}(2\overline{H}/\sqrt{D\bar{\tau}})} \tag{8}$$

Reverting back into y domain the desired surface rejuvenation based system of equations for mean profiles $\bar{\phi}$ and $\overline{C}$ becomes

$$\frac{\bar{\phi}-\phi_\infty}{\phi_w-\phi_\infty} = \frac{J_{2\overline{H}/\sqrt{\Im\bar{\tau}}}(2\overline{H}/\sqrt{\Im\bar{\tau}}e^{-y/2\overline{H}})}{J_{2\overline{H}/\sqrt{\Im\bar{\tau}}}(2\overline{H}/\sqrt{\Im\bar{\tau}})} \tag{9}$$

$$\frac{\overline{C}-C_\infty}{C_w-C_\infty} = e^{(\overline{V}_t/D)y}\frac{J_{\sqrt{(2\overline{H}/\sqrt{D\bar{\tau}})^2+(\overline{H}\overline{V}_t/D)^2}}(2\overline{H}/\sqrt{D\bar{\tau}}e^{-y/2\overline{H}})}{J_{\sqrt{(2\overline{H}/\sqrt{D\bar{\tau}})^2+(\overline{H}\overline{V}_t/D)^2}}(2\overline{H}/\sqrt{D\bar{\tau}})} \tag{10}$$

The algorithm of Bessel function $J_n(x)$ is based on a code due to [25] that uses backward recursion with strict error control and the order of Bessel function n has to be a positive integer. Therefore, during the numerical predictions as will be performed below, the transport parameters of 2υ, 2ϑ and ϖ act as the order of Bessel function must be designated as positive integers.

3.1. Mean eddy approach distance

With the boundary conditions $\bar{u}=0$ at $y=0$ and $\bar{u}=u_\infty$ at $y\to\infty$ of Eq. (9), the mean velocity distribution can be obtained by

$$\frac{\bar{u}-u_\infty}{-u_\infty} = \frac{J_{2\upsilon}(2\upsilon e^{-y/2\overline{H}})}{J_{2\upsilon}(2\upsilon)} \tag{11}$$

where $\upsilon = \overline{H}/\sqrt{\nu\bar{\tau}}$ is the transport parameter and ν is the kinematic viscosity. The mean wall shear stress, $\bar{\sigma}_w = \mu\partial\bar{u}/\partial y|_{y=0}$ can then be written as

$$\bar{\sigma}_w = \frac{\mu u_\infty}{\sqrt{\nu\bar{\tau}}}\left(\frac{J_{2\upsilon-1}(2\upsilon)-J_{2\upsilon}(2\upsilon)}{J_{2\upsilon}(2\upsilon)}\right) \tag{12}$$

where μ is the dynamic viscosity. In accordance with the Blasius resistance formula the expression for the mean shear stress at the wall is $\bar{\sigma}_w = \rho u_*^2 = 0.0268\rho u_\infty^2 Re^{-1/4}$, where $Re = u_\infty d/\nu$ based on substituting the mean velocity $\bar{u}$ with the aid of the maximum velocity u_∞ by putting $\bar{u}=0.8u_\infty$ [26]. Rearranging Eq. (12) eliminates the effect of pipe diameter, d, and gives

$$\Re = \frac{Re^{-3/4}\upsilon}{0.0268}\left(\frac{J_{2\upsilon-1}(2\upsilon)-J_{2\upsilon}(2\upsilon)}{J_{2\upsilon}(2\upsilon)}\right) \tag{13}$$

where $\Re = \overline{H}/d$ represents the dimensionless mean eddy approach distance from the pipe wall as functions of Reynolds number and transport parameter υ for all radial fluctuation fractions of turbulent fluid, and also provides the solution for the dimensionless mean residence time $\bar{\tau}^+ = u_*\sqrt{\bar{\tau}/\nu}$ while the dimensionless pipe diameter is calculated by $d^+ = du_*/\nu = 0.1637Re^{7/8}$ [27].

3.2. Mean thermophoresis velocity

In many theoretical literatures provided analytical formulas for the thermal force acting on small spherical particles, the thermal force is usually transformed into thermophoretic velocity based on the balance between the drag force and thermal force while the inertia force was ignored. The equation of the thermophoretic velocity, $V_t = -k\nu/T\,\partial T/\partial y$, proposed by [28] is widely accepted and the same expression is adopted in the present research for predicting the mean thermophoretic velocity coefficient $V_{\text{th}} = \overline{V}_t\overline{H}/\alpha$. The mean temperature gradient is calculated according to the boundary conditions $\overline{T}=T_w$ at $y=0$ and $\overline{T}=T_\infty$ at $y\to\infty$ of Eq. (9), and is given in [9] as

$$\frac{\overline{T}(y)-T_\infty}{T_w-T_\infty} = \frac{J_{2\vartheta}(2\vartheta e^{-y/2\overline{H}})}{J_{2\vartheta}(2\vartheta)} \tag{14}$$

where the transport parameter $\vartheta = \overline{H}/\sqrt{\alpha\bar{\tau}}$ indicates the comparable intensities between the thermal and turbulent mechanism. Under fixed value of υ it acts as Prandtl number $Pr = \nu/\alpha$ to adjust the incidences of thermal and turbulent structure in the wall region, where the thickness of thermal boundary layer and the radial turbulent influence are usually varying with ϑ. As a result of surface rejuvenation model, the mean thermophoretic velocity coefficient V_{th} can be calculated by

$$V_{\text{th}} = \frac{k\vartheta^3}{\upsilon^2}\left(\frac{T_w-T_\infty}{T_\infty}\right) \times \left(\frac{e^{-(1/(2\Re))Y}J_{2\vartheta-1}[2\vartheta e^{-(1/(2\Re))Y}] - J_{2\vartheta}[2\vartheta e^{-(1/(2\Re))Y}]}{J_{2\vartheta}[2\vartheta]+((T_w-T_\infty)/T_\infty)J_{2\vartheta}[2\vartheta e^{-(1/(2\Re))Y}]}\right) \tag{15}$$

where $Y = y/d$ is the dimensionless distance measured normal to the wall. The thermophoretic coefficient k generally depends on particle size as function of the Knudsen number K_n and the following formula has been widely applied in the entire range of Knudsen number [28].

$$k = \frac{2C_sC_f(K_g/K_p + C_tK_n)}{(1+3C_sK_n)(1+2K_g/K_p+C_tK_n)} \tag{16}$$

where $C_s = 1.147$ is the thermal slip coefficient, $C_t = 2.18$ the temperature jump coefficient, and $C_m = 1.146$ the momentum exchange coefficient [29]. K_g and K_p are the thermal conductivities of the carrier gas and the particle, respectively. C_f represents the Cunningham slip correction factor and is obtained by $C_f = 1 + K_n(1.257 + 0.4e^{-1.1/K_n})$ [30]. The Knudsen number $K_n = \lambda/r_p$, defined as the ratio of the molecular mean free path of an aerosol particle λ to the radius of the spherical particle r_p, is generally used to characterize the interaction of gases and particles during the analysis of thermophoretic coefficient k

which is linearly increased with increasing K_n in the continuum regime ($K_n \ll 1.0$) and hyperbolically increased in transition regime ($K_n \approx 1.0$). In the free molecular regime ($K_n \gg 1.0$) the thermophoretic coefficient is not affected by the thermal conductivity ratio and trends to a constant value of $k = 0.55$, but it is seen to be slightly lower than 0.55 at $K_n > 1.0$ in the experimental data of Messerer et al. [18].

3.3. Mean deposition velocity

Solutions of the momentum and energy equations yield the velocity and temperature distributions in the boundary layer and these are used in the coupled concentration equation to calculate the rates of particle deposition. Based on Eq. (10) the dimensionless mean concentration distribution on the wall can be obtained by

$$\frac{\overline{C} - C_\infty}{C_w - C_\infty} = e^{(V_{\mathrm{th}}\omega^2/(2\Re\vartheta^2))Y} \times \frac{J_{\sqrt{(2\omega)^2+(V_{\mathrm{th}}\omega^2/\vartheta^2)^2}}(2\omega e^{-(1/(2\Re))Y})}{J_{\sqrt{(2\omega)^2+(V_{\mathrm{th}}\omega^2/\vartheta^2)^2}}(2\omega)} \quad (17)$$

where $\omega = \overline{H}/\sqrt{D\bar{\tau}}$ is a transport parameter which links the turbulent contribution to the particle transport processes, under fixed value of υ it acts as Schmidt number $Sc = \nu/D$ and can be obtained in accordance with the calculated value of V_{th}.

In turbulent flow the eddies are not the final mechanism for impaction on the surface since turbulence decays to zero in the vicinity of the surface. Most of the theories assume that the particles move toward the wall by perpendicular motion only, and that the deposition flux of particles, N, is obtained by assuming equality between eddy diffusivity of the fluid and particle diffusivity. In accordance with equation (17) the mean mass transport flux can be expressed as $\overline{N} = -D\partial\overline{C}/\partial y|_{y=0}$, and subsequently the mean thermophoretic transport coefficient can be estimated by

$$\frac{\overline{V}_d\overline{H}}{D} = -\overline{H}\frac{\partial\frac{\overline{C}-C_w}{C_\infty-C_w}}{\partial y}\bigg|_{y=0} = \left(\omega\frac{J_{\sqrt{(2\omega)^2+(V_{\mathrm{th}}\omega^2/\vartheta^2)^2}-1}(\omega^{1/2})}{J_{\sqrt{(2\omega)^2+(V_{\mathrm{th}}\omega^2/\vartheta^2)^2}}(\omega^{1/2})} - \frac{\sqrt{(2\omega)^2+(V_{\mathrm{th}}\omega^2/\vartheta^2)^2}}{2} - \frac{1}{2}\frac{\overline{V}_t\overline{H}}{\alpha}\left(\frac{\omega}{\vartheta}\right)^2\right) \quad (18)$$

4. Results and discussions

The radial fluctuation fractions of turbulent fluid intermittently move from the turbulent core to near the wall, $\upsilon = \overline{H}/\sqrt{\nu\bar{\tau}}$ is a dominating parameter for characterizing the radial fluid inertia as well as the mean approach distance of eddy $\overline{H}/d$ and the dimensionless mean residence time $\bar{\tau}^+$, which can calculated by the velocity distribution in the fully turbulent fluid flow derived from the surface rejuvenation model. $\bar{\tau}^+$ compared with previously measured values of visual flow studies [5] is shown in Fig. 2 as a function of the transport parameter υ and Reynolds number Re. The visual flow studies indicate that $\bar{\tau}^+$ is $14 \leqslant \bar{\tau}^+ \leqslant 17$ in the smooth tube flows for $2 \times 10^4 < Re < 5.5 \times 10^4$. Calculated $\bar{\tau}^+$ obviously deviates from the visual flow studies by an increase in the value of υ, but a correct value of the transport parameter $\upsilon = 0.5$ seems quite satisfactory. As a result of the present studies, the dimensionless mean residence time of viscous sublayer is $13.088 \leqslant \bar{\tau}^+ \leqslant 19.032$ in the smooth tube flows for $5 \times 10^3 < Re < 1.0 \times 10^5$, and $\bar{\tau}^+$ near a constant at high Reynolds number agrees with the sublayer model where the dimensionless mean residence time was essentially constant around 18.0 for Reynolds number greater than 10^4 [31].

In the manner of the surface rejuvenation model the dimensionless mean thermophoretic velocity $V_{\mathrm{th}} = \overline{V}_t\overline{H}/\alpha$ is employed to specify the thermophoretic effect. Since the Knudsen number gets larger as the particle diameter gets smaller, the calculated value of V_{th} at $Y = 0.0$, where the temperature gradient is the greatest, relative to Knudsen number is reflected in Fig. 3 by directly plotting V_{th} against Schmidt number Sc for the specified values of the thermal conductivity ratio K_g/K_p. The calculated value of V_{th} maintains constant for smaller particles as ranged in the free molecular regime, but it is always lower at larger particles with slightly decreasing as particle diameter is increased. The thermal conductivity effect on the dimensionless mean thermophoretic velocity agrees with the theoretical results [32] and the experimental measurements [18], they indicated

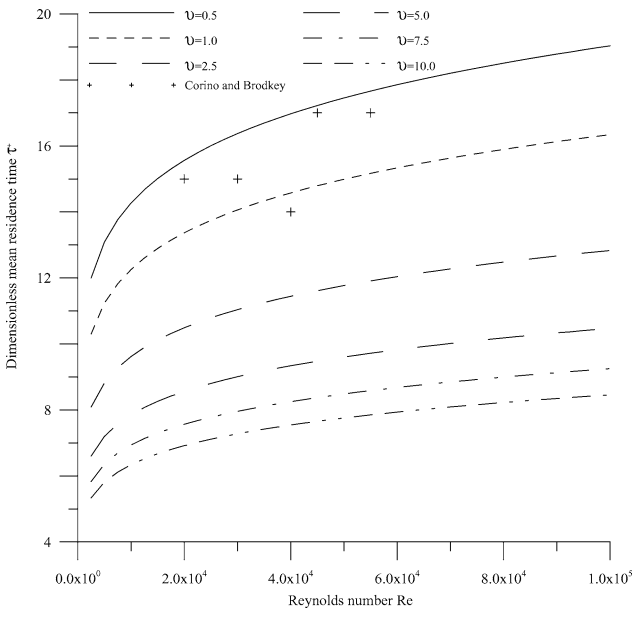

Fig. 2. Dimensionless mean sublayer residence time as function of transport parameter υ and Reynolds number.

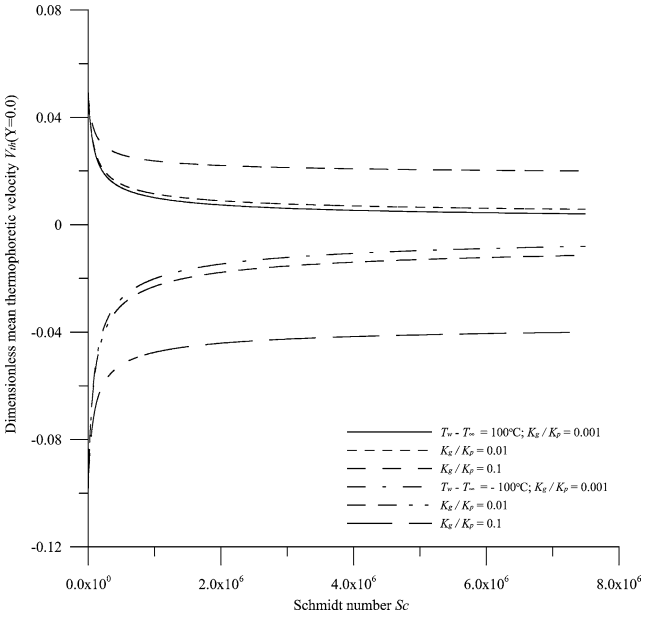

Fig. 3. Calculated value of V_{th} at $Y = 0.0$ as function of Schmidt number and thermal conductivity at $\vartheta = 0.5$, $\upsilon = 0.5$, $Re = 5.0 \times 10^4$, $Sc = 2.598 \times 10^4$ and $\rho_p/\rho_g = 1{,}000$.

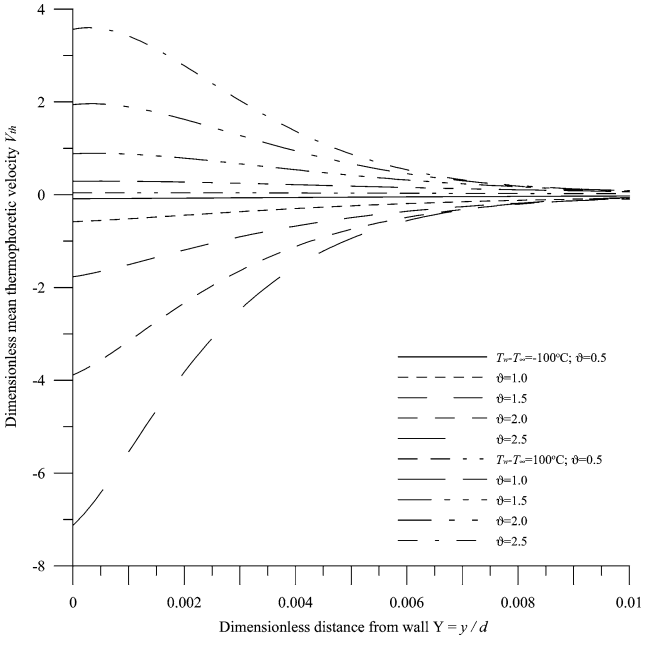

Fig. 4. Distribution of dimensionless mean thermophoretic velocity related to transport parameter ϑ at $\upsilon = 0.5$, $Re = 5.0 \times 10^4$, $Sc = 2.598 \times 10^4$, $K_g/K_p = 0.1$ and $\rho_p/\rho_g = 1{,}000$.

that the thermophoretic coefficient and velocity can be significantly enhanced by reducing the thermal conductivity of the aerosol particles. Fig. 4 describes the distribution of mean thermophoretic velocity V_{th} for the specified values of $\vartheta = \overline{H}/\sqrt{\alpha\bar{\tau}}$. Based on the surface rejuvenation model, the transport parameter ϑ acted as a main factor on the thermophoretic effect is a dominating parameter for characterizing the turbulent contribution to the thermal energy. The

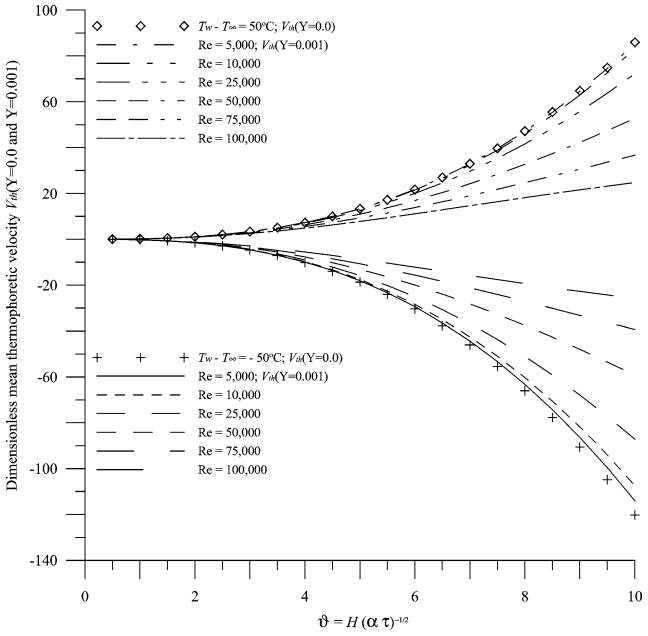

Fig. 5. Calculated value of V_{th} at $Y = 0.0$ related to Reynolds number and transport parameter ϑ at $\upsilon = 0.5$, $Sc = 2.598 \times 10^4$, $K_g/K_p = 0.1$ and $\rho_p/\rho_g = 1{,}000$.

calculated value of V_{th} at $Y = 0.0$ is significantly affected with varying ϑ because it is determined from the conditions near the wall where the fluctuating sublayer imposes the wall temperature fluctuations resulting in varying thickness of the thermal boundary layer. At high value of ϑ, the outer edge of the growing sublayer is always farther from the wall than the penetration of the thermal wave during a growth cycle and the high thermal fluctuation gets closer to the surface where the difference of the thermophoretic effects widens. At low value of ϑ, the thermal fluctuations adhere to the velocity fluctuations of the fluid and the thermal transfer due to turbulence is limited by the boundary layer. It is interesting that the distribution of V_{th} has clearly indicated the influence of thermal force inside the viscous sublayer, and that the turbulent eddy diffusion do cause an alteration in thermal diffusion near the heating surface and an enhancement near the cooling surface. Following, the relationship between V_{th} and ϑ is built to gain more insight into the effect of thermophoresis as shown in Fig. 5 where the calculated value of V_{th} at $Y = 0.001$ is plotted against the transport parameter ϑ and closely related to the control of the flow eddies near the wall region by varying mainstream velocities. A comparable case is modeled with the calculated wall value where ϑ is the only mechanism to affect the thermal transfer processes. The calculated value of V_{th} at $Y = 0.001$ decreases and deviates from the wall value with increasing Reynolds number, whereas it come near the wall value at low Reynolds number where the viscous boundary layer drags the surrounding fluid and prevents the flow from taking more heat. Clearly, at high values of ϑ the thermal boundary maintains itself close to the wall resulting in enhancing the thermophoretic effect,

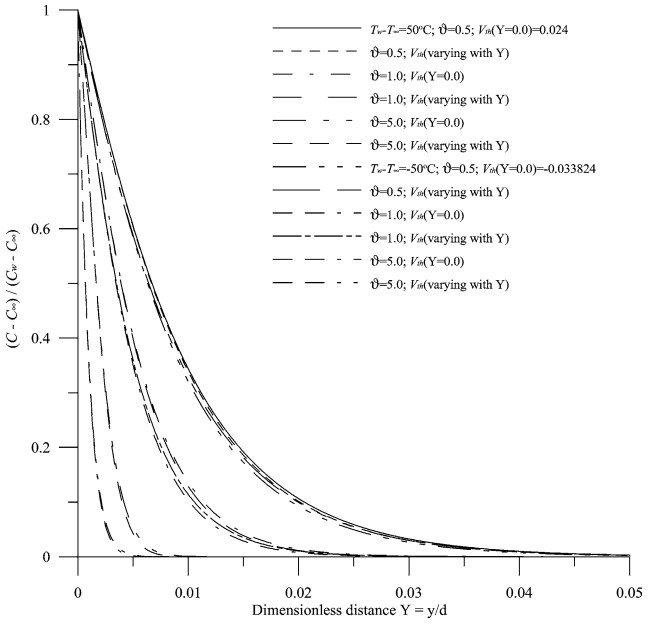

Fig. 6. Comparison of dimensionless mean concentration distribution between constant V_{th} at $Y = 0.0$ and V_{th} varying along Y.

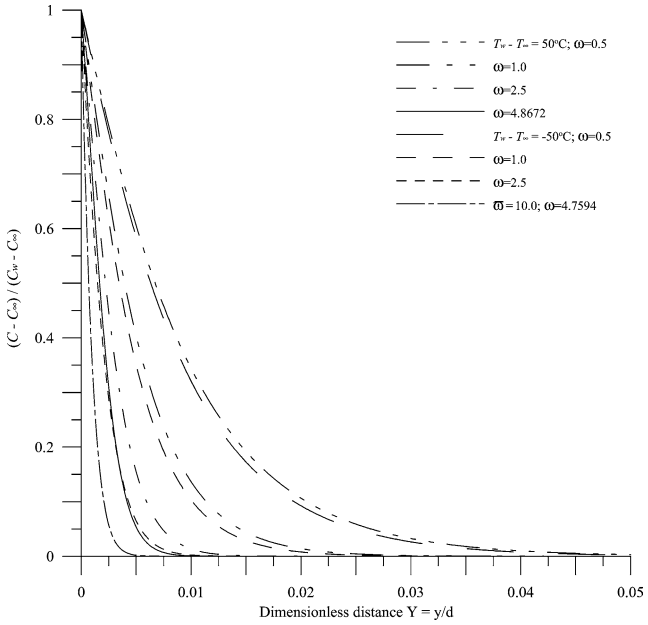

Fig. 7. Dimensionless mean concentration distribution for lower values of ω at $\vartheta = 0.5$, V_{th} $(Y = 0.0)$, $\upsilon = 0.5$, $Re = 5.0 \times 10^4$ and $Sc = 2.598 \times 10^4$.

while at low ϑ it spreads over the whole thickness of viscous sublayer.

In general, the particles suspended in the turbulent fluid would tend to collect in the sublayer since the turbulent eddies become steadily weaker as the surface is approached and the turbulent eddy diffusion may has no effect upon the transfer process, thus the thermal mechanism existed in the wall region may play a coherent role to enhance the particle transfer processes in the viscous wall region, especially for the particles with small molecule diffusion. The sublayer oscillations impose a wall temperature fluctuation and the concentration distribution has to be solved simultaneously. According to Eq. (17) the thermophoretic velocity is the coupling factor to perform this simulation as shown in Fig. 6 involving a comparable case modeled with the calculated value of V_{th} at $Y = 0.0$. The results indicate that there is no really significant difference between two conditions of V_{th}. It means that the turbulent fluctuations almost certainly do not penetrate completely to the wall, and that the conditions at the outer edge of the sublayer are not too important on the transfer processes. In Figs. 7 and 8, the transport parameter ω derived from surface rejuvenation model is used to characterize the turbulent contribution to the concentration development under a fixed structure of thermal boundary layer $\vartheta = 0.5$. The concentration development retarded by the viscous sublayer leads to a significant decrease in concentration gradient at low values of ω. Whereas its growth rate certainly increases with an increase in ω, especially near the cooling surface where the turbulence gives much more contribution to the growth rate and causes that the thickness of concentration boundary layer is always thinner to some extent than that of heating surface. It is interesting that the concentration growth rates on the cooling surface always vary with the

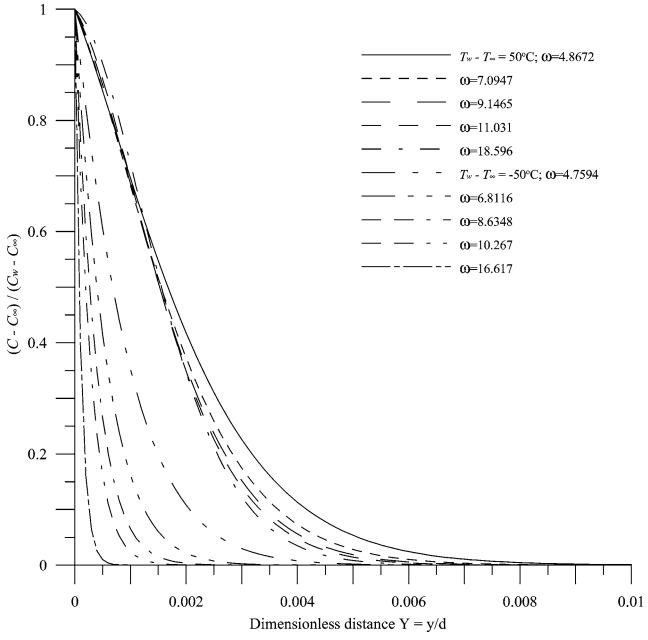

Fig. 8. Dimensionless mean concentration distribution for higher values of ω at $\vartheta = 0.5$, V_{th} $(Y = 0.0)$, $\upsilon = 0.5$, $Re = 5.0 \times 10^4$ and $Sc = 2.598 \times 10^4$.

transport parameter ω, whereas more disturbances come to near the heating wall, especially at high values of ω as showing Fig. 8. At $\omega \geqslant 5.0$, the reverse thermophoresis pushes the concentration boundary layer away from the heating surface while the radial turbulence fluctuation propels it toward the wall. These two mechanisms acted against each other cause an upturned trend near the heating surface resulting in bring down the concentration gradient, thus reducing the transfer rate as will be discussed below.

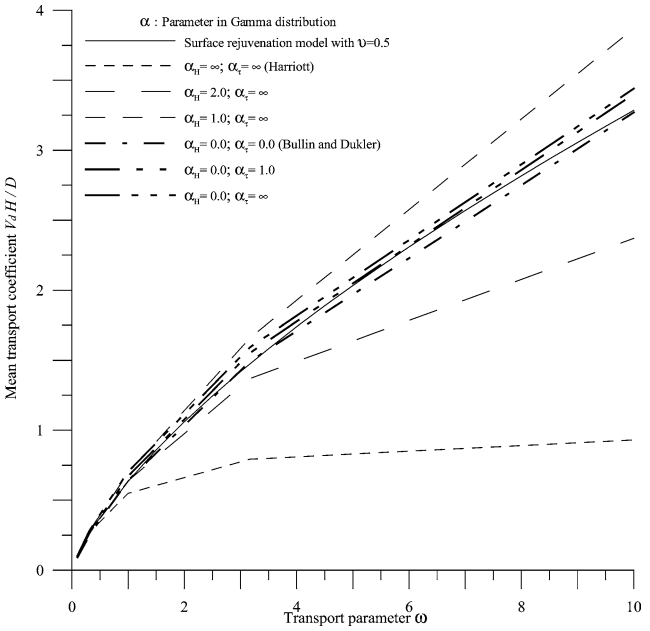

Fig. 9. Compared mean transport rate with previously proposed models in isothermal turbulence fluid flow.

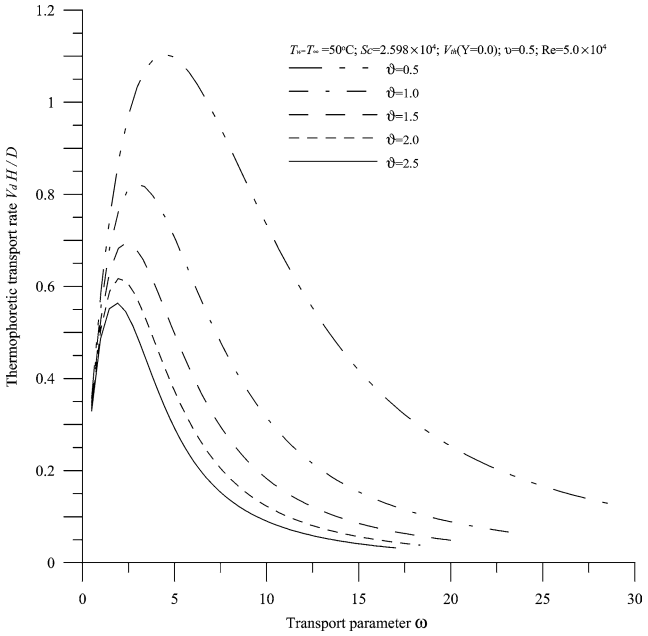

Fig. 10. Calculated value of dimensionless mean thermophoresis transport rate at heating surface depends on transport parameters ω and ϑ.

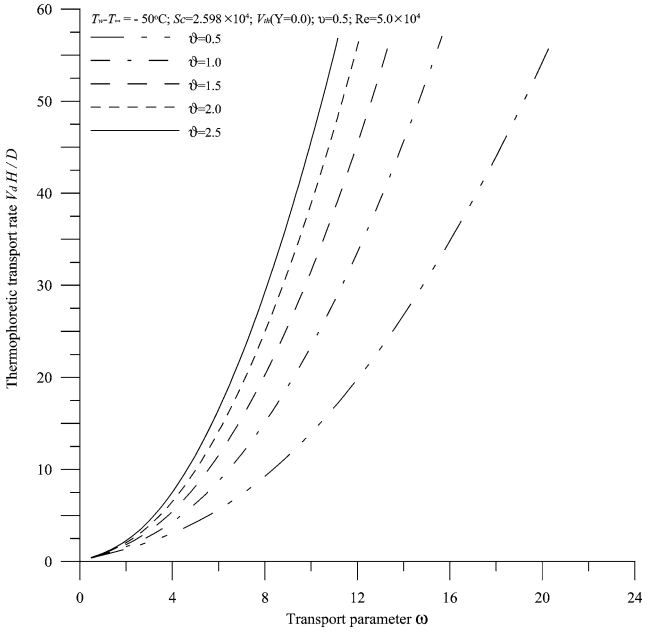

Fig. 11. Calculated value of dimensionless mean thermophoresis transport rate at cooling surface depends on transport parameters ω and ϑ.

Fig. 9 shows the comparison of the dimensionless mean particle transport rate $\overline{V}_d\overline{H}/D$ with previously proposed models [7,8]. The results of the modified Danckwert model for the dimensionless mean particle transport rate in terms of unspecified modeling parameters $\bar{\tau}$ and $\overline{H}$ are based on varying a single parameter α of gamma density to obtain different statistical distributions. In Harriott's results, the dimensionless mean particle transport rate is changed dramatically at high value of ω with the varying distribution form of the eddy approach distance ($\alpha_H = \infty, 2, 1$) while the renewal time was held constant ($\alpha_\tau = \infty$). The same conclusion appears in Bullin's results for variable α_τ while the eddy approach distance was held on to a fixed distribution form $\alpha_H = 0$. The present result is seen to be in good agreement except $\alpha_H = \infty$ corresponding to the constant approach distance which is expected to be applied at low $\omega = \overline{H}/\sqrt{D\bar{\tau}}$ as the penetration theory.

In a nonisothermal turbulence flow field, a comparable coupling between the thermal and turbulent mechanism may significantly dominate the particle transport processes in regions close to the wall, and thus the particle transport rate at the interface may generally be affected by the combined action of molecular diffusion, turbulence, and thermophoresis. These are shown in Figs. 10 and 11 where the calculated values of the dimensionless mean thermophoretic transport rate $\overline{V}_d\overline{H}/D$ at $Y = 0.0$ are plotted against ω for the specified values of ϑ. At the heating surface, the thermophoretic transport rate increases not only with increasing ω but also with decreasing ϑ. The increase of concentration gradient extends to some extent along with ω giving rise to an increase in the thermophoretic transport rate which relatively reaches its peak at the value of ω right before that the upturned tendency of concentration profile comes into existence as shown in Fig. 8. The peak value varying with the specified values of ϑ validates that the appearance of upturned tendency will begin at the different value of ω according to the specified value of ϑ, and that the turbulence takes command of total transport rate at lower values of ω where the concentration fluctuation tends to follow the velocity fluctuation of the fluid more closely, while the thermal transfer is limited by the boundary layer at low values of ϑ. The thickness of the growing sublayer is always farther from the wall than the penetration concentration wave during a growth cycle at

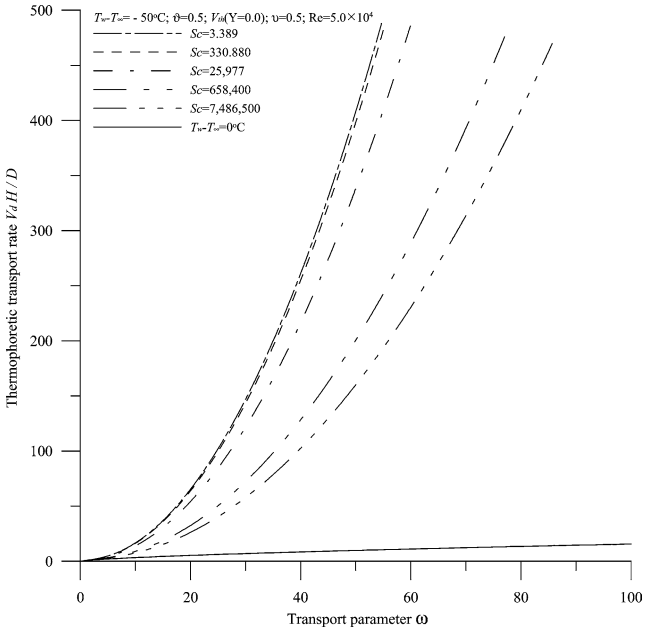

Fig. 12. Calculated value of dimensionless mean thermophoresis transport rate at cooling surface depends on transport parameters ω and Schmidt number.

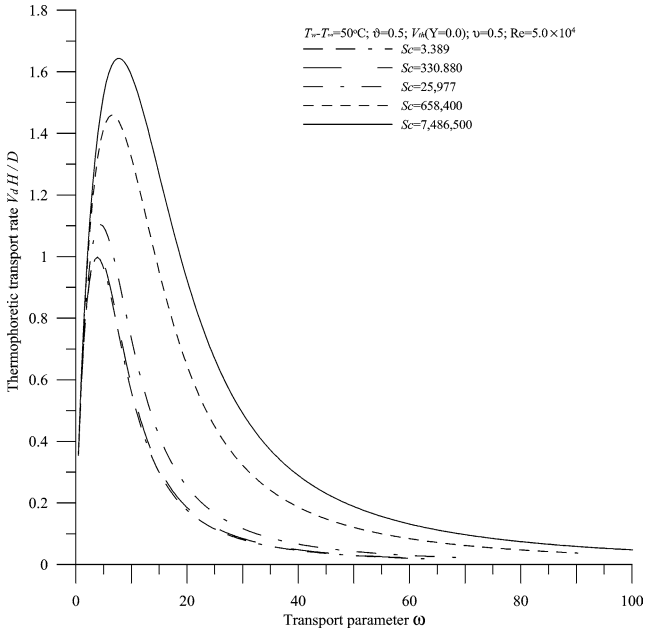

Fig. 13. Calculated value of dimensionless mean thermophoresis transport rate at heating surface depends on transport parameters ω and Schmidt number.

higher values of ω. The thermal energy is high in the region close to the wall at higher values of ϑ and is transported from the heating surface to the bulk flow. The thermophoresis balances against the turbulence in the wall region giving rise to a decrease in the total transport rate after the pick value and the particle transport rate may approach a constant value as the wall disturbance increases further. At the cooling surface, thermophoresis enhances the coherent effect of turbulence and molecular diffusion to diffuse the particles through the viscous sublayer during the random sequences of eddy lifetimes resulting in a significant increase in the thermophoretic transport rate which increases with the increases in both ω and ϑ. This result can also be felt out by following the thread of the concentration profile where the concentration gradient increases not only with increasing ω but also with increasing ϑ, which means that the depth of penetration of the concentration boundary layer is strongly dependent on both of them.

Subsequently, Figs. 12 and 13 indicate the effect of molecular diffusion on the particle transfer processes during the mean residence time of turbulent sublayer. In an isothermal turbulence flow field, the relative velocity between particles and fluid tends to increase as particle diameter increases, and the interaction of larger particles with the wall structures is greater near the wall giving rise to an enhancement of wall viscosity, whereas the smaller particles cause a suppression of this intensity. The results indicate that a pronounced increase in the transport rate appears as compared with the isothermal profile. A coherent enhancement on the molecular diffusion caused by turbulence and thermophoresis is found to play an important role in the particle transport process throughout the particle diameters considered. The slope of the transport rate decays with decreasing molecular diffusion, this is in contrast to the case of the heating surface as shown in Fig. 13 where the thermophoretic effect on the total transport rate is most important for low diffusivities, and appears not so conspicuous for the smaller particles conducing to the steeper slope of the transport rate on the larger particles. Based on the above results, the slope of decay of the transport rate depends on not only the turbulent structure in the wall region but also the particle diameter and the thermophoretic effect. The effect of the thermophoresis are more significant for larger particles than for the smaller particles at the heating surface and the contrary results appear at the cooling surface where the calculated values of thermophoretic transport rate are much higher than the heating surface.

5. Conclusion

The approximate analysis solutions have been obtained for predicting the viscous sublayer, thermophoretic effect and transport rate in detail. The dimensionless mean residence time of viscous sublayer based on the surface rejuvenation model is $13.088 \leqslant \bar{\tau}^+ \leqslant 19.032$ in the smooth tube flows for $5 \times 10^3 < Re < 1.0 \times 10^5$ which is consistent with visual observations. The calculated values of dimensionless mean thermophoresis velocity V_{th} maintain constant for smaller particles as ranged in the free molecular regime independent of the thermal conductivity ratio, but they are always lower at larger particles, slightly decrease with increasing particle diameters and seen to be sensitive to the thermal conductivity ratio. A comparable coupling between

the thermal and turbulent mechanism significantly dominates the thermophoretic effect in regions close to the wall where the calculated values of V_{th} at $Y = 0.0$ extend from the heating surface to some extent and the amplitude spread of V_{th} profiles is rather broad, especially at low Reynolds number. A clear coupling on the particle transfer mechanisms near the wall provides a good agreement of mean transport rate in an isothermal turbulence fluid flow as compared with previous models which proves the subsequent development of the interactions between thermal and turbulent mechanism on the particle transport processes.

The entire transfer processes take place inside the sublayer created by the radial turbulence eddies which repeat itself causing the migration of turbulent energy from the bulk flow to the wall region. The concentration profiles plotted under different conditions of thermophoretic velocity shows that the eddies do not penetrate completely to the wall, and that the conditions at the out edge of the sublayer can be neglected during the transfer processes. Therefore, the transport of particles in the flow direction mostly accumulates in low speed streak near the interacting region. Coherent temperature gradients existed in the wall region would be the only mechanism to enhance the particle transport rate, because the increase in temperature gradient can dramatically increase the thermophoretic effect by directly reforming the thermal structure inside the viscous sublayer where a thermal boundary disturbs not only the local concentration field but also the viscous sublayer experienced by the particles, which causes the thermophoretic behavior of the particle to deviate from its behavior when it is in the isothermal flow field. The deviation is observed to be greater near the cooling surface where the effects of coherent mechanisms acted conjunctively on the enhancement of the particle transport rates are always higher for smaller particles.

The concentration gradients extended from the heating surface to some extent cause the upturn tendencies of concentration profiles. The mean transport rates increasingly reach their peak values right after the upturn came into existence depending on the comparable effects of thermal and turbulent mechanism, and then reduce to approach a constant value as the wall disturbance increases. The relative velocity increase with an increase in particle diameter and it is largest near the heating surface where the thermal energy is transported from the wall region to the bulk flow. The response of the larger particles to the fluid velocity decreases giving rise to an increase in the relative velocities and transport rates. The smaller particles tend to follow the flow more closely, though there is still a relative velocity between the particle and the fluid.

References

[1] C. Kroger, Y. Drossinos, A random-walk simulation of thermophoretic particle deposition in a turbulent boundary layer, Internat. J. Multiphase Flow 26 (2000) 1325–1350.

[2] C. Greenfield, G. Quarini, A Lagrangian simulation of particle deposition in a turbulent boundary layer in the presence of thermophoresis, Appl. Math. Modelling 22 (1998) 759–771.

[3] S.A. Slater, A.D. Leeming, J.B. Young, Particle deposition from two-dimensional turbulent gas flow, Internat. J. Multiphase Flow 29 (2003) 721–750.

[4] M. Shin, D.S. Kim, J.W. Lee, Deposition of inertia-dominated particles inside a turbulent boundary layer, Internat. J. Multiphase Flow 26 (2003) 892–926.

[5] E.R. Corino, R.S. Brodkey, A visual investigation of the wall region on turbulent flow, J. Fluid Mech. 37 (1969) 1–30.

[6] M. Rashidi, G. Hetsron, S. Banerjee, Particle-turbulence interaction in a boundary layer, Internat. J. Multiphase Flow 16 (1990) 935–949.

[7] P. Harriott, A random eddy modification of the penetration theory, Chem. Engrg. Sci. 17 (1962) 149–154.

[8] J.A. Bullin, A.E. Dukler, Random eddy models for surface renewal: formulation as a stochastic process, Chem. Engrg. Sci. 27 (1972) 439–442.

[9] L.C. Thomas, P.J. Gingo, B.T.F. Chung, The surface rejuvenation model for turbulent convective transport—an exact solution, Indust. Engrg. Chem. Fund. 10 (1975) 1239–1242.

[10] L.C. Thomas, The surface rejuvenation model of wall turbulence: Inner laws for u^+ and T^+, Internat. J. Heat Mass Transfer 23 (1980) 1099–1104.

[11] S. Brocker, A new viscous sublayer influx (VSI) concept for near-wall turbulent momentum, heat and mass transfer, Rev. Gen. Therm. 37 (1988) 353–370.

[12] B. Singh, R.L. Byers, Particle deposition due to thermal force in the transition and near-continuum regimes, Indust. Engrg. Chem. Fundam. 11 (1972) 127–133.

[13] S.L. Goren, Thermophoresis of aerosol particles in laminar boundary layer of a flat plate, J. Colloid Interface Sci. 6 (1977) 77–80.

[14] J.S. Chang, T. Ishii, S. Matsumura, S. Ono, S. Teii, Theory of aerosol particle thermal deposition on flat body in a variable property fluid, J. Aerosol Sci. 18 (1987) 619–621.

[15] P. Han, T. Yoshida, Modeling of clusters deposition under the effect of thermophoresis during thermal plasma flash evaporation process, Sci. Tech. Adv. Materials 2 (2001) 367–374.

[16] M.C. Chiou, Sub-micron particle deposition on an isothermal horizontal rod in a turbulent flow system, Acta Mech. 145 (2000) 135–158.

[17] L. Waldmann, K.H. Schmitt, Thermophoresis and diffusiophoresis of aerosol, in: C.N. Davies (Ed.), Aerosol Science, Academic Press, London, 1966.

[18] A. Messerer, R. Niessner, U. Poschl, Thermophoretic deposition of soot aerosol particles under experimental conditions relevant for modern diesel engine exhaust gas systems, J. Aerosol Sci. 34 (2003) 1009–1021.

[19] J.S. Lin, C.J. Tsai, Thermophoretic deposition efficiency in a cylindrical tube taking into account developing flow at the entrance region, J. Aerosol Sci. 34 (2003) 569–583.

[20] C.H. Chiu, C.M. Wang, M.C. Chiou, Thermophoretic effects on submicron particle deposition in turbulent flow, Acta Mech. 170 (2004) 213–226.

[21] P.V. Danckwerts, Significance of liquid-film coefficients in gas absorption, Indust. Engrg. Chem. 43 (1951) 1460–1467.

[22] T.J. Hanratty, Turbulent exchange of heat and momentum with a boundary, AIChE J. 2 (1956) 359–362.

[23] J.M.H. Fortuin, E.E. Musschenga, P.J. Hamersma, Transfer processes in turbulent pipe flow described by the ERSR model, AIChE J. 38 (1992) 343–362.

[24] E.E. Musschenga, P.J. Hamersma, J.M.H. Fortuin, Momentum, heat and mass transfer in turbulent pipe flow: The extended random surface renewal model, Chem. Engrg. Sci. 47 (1992) 343–362.

[25] D.J. Sookne, Bessel functions of real argument and integer order, National Bureau Standards J. Res. B 77A (1973) 125–132.

[26] H. Schlichting, Boundary-Layer Theory, seventh ed., McGraw-Hill, New York, 1979.
[27] B. Eck, Technische Stromungslehre, Springer, New York, 1973.
[28] L. Talbot, R.K. Cheng, R.W. Schefer, D.R. Willis, Thermophoresis of particles in a heated boundary layer, J. Fluid Mech. 101 (1980) 737–758.
[29] G.K. Batcheler, C. Shen, Thermophoretic deposition of particles in gas flowing over cold surfaces, J. Colloid Interface Sci. 107 (1985) 21–37.
[30] S.H. Friedlander, Smoke, Dust and Haze-Fundamentals of Aerosol Behavior, Wiley, New York, 1977.
[31] R.L. Meek, A.D. Baer, The periodic viscous sublayer in turbulent flow, AIChE J. 16 (1970) 841–848.
[32] D.E. Rosner, Y.F. Khalil, Particle morphology and Knudsen number transition-effects on thermophoretically dominated total mass deposition rates from “coagulation-aged” aerosol population, J. Aerosol Sci. 31 (2000) 273–292.